
INFERRING ASTROPHYSICAL X-RAY POLARIZATION WITH DEEP LEARNING

Nikita Moriakov

Radiology, Nuclear Medicine and Anatomy
Radboud University Medical Center
Nijmegen, Netherlands
nikita.moriakov@radboudumc.nl

Ashwin Samudre

Aix-Marseille-Univ, CNRS, CINAM
Marseille, France
ashwin.samudre@cinam.univ-mrs.fr

Michela Negro

NASA-GSFC/CRESST-UMBC
Greenbelt, MD 20771, USA
michela.negro@nasa.gov

Fabian Gieseke

Department of Computer Science
University of Copenhagen
Copenhagen, Denmark
fabian.gieseke@di.ku.dk

Sydney Otten

University of Amsterdam and
Radboud University Nijmegen
s.m.m.otten@uva.nl

Luc Hendriks

Radboud University
Nijmegen, the Netherlands
luc@luchendriks.com

DarkMachines collaboration: darkmachines.org. **Particle Track Reconstruction with ML Group.**

ABSTRACT

We investigate the use of deep learning in the context of X-ray polarization detection from astrophysical sources as will be observed by the Imaging X-ray Polarimetry Explorer (IXPE), a future NASA selected space-based mission expected to be operative in 2021. In particular, we propose two models that can be used to estimate the impact point as well as the polarization direction of the incoming radiation. The results obtained show that data-driven approaches depict a promising alternative to the existing analytical approaches. We also discuss problems and challenges to be addressed in the near future.

1 Introduction

The *Imaging X-ray Polarimetry Explorer*¹ (IXPE), which is a space-based mission selected by the NASA, is expected to be launched in 2021. IXPE will conduct precise polarimetry in the X-ray energy band (between 2 and 8 kilo electronvolts), which is a poorly investigated field so far, see (Weisskopf, 2018) for a recent review. The data collected by this mission will be important for the analysis of various astrophysical sources, from stellar-mass black holes, neutron stars and pulsar wind nebulae, to supernovae remnants and active galactic nuclei.

IXPE exploits the so-called *Gas Pixel Detector* (GPD) design to perform measurements of linear polarization (Bellazzini et al., 2006). In particular, when an X-ray photon is absorbed in the gas gap of the GPD, a photo-electron (PE) is ejected, producing an ionization pattern that defines a track. Each track is drifted by a uniform electric field to the *Gas Electron Multiplier* (GEM), which amplifies the charge keeping the shape unchanged (Costa et al., 2001). The amplified charge is then read out through a grid of hexagonal pixels and the image of the PE is recorded. An example of a PE track image is given in Figure 1: the green dot represents the impact point, where the X-ray converted into a PE,

¹<https://ixpe.msfc.nasa.gov>

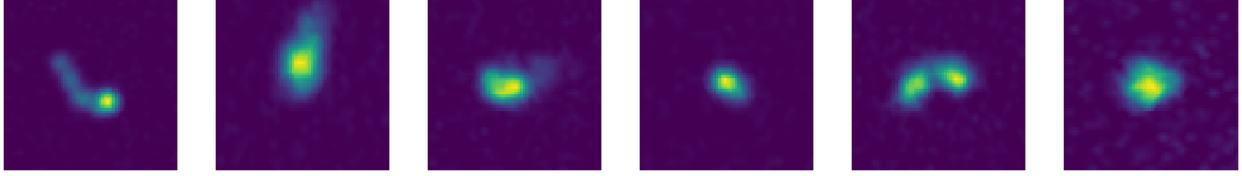


Figure 2: Examples of simulated images

and the green line shows the emission direction of the secondary particle, which lies preferentially in the oscillation plane of the X-ray electric field.

A correct reconstruction of the impact point is crucial to carry out the imaging of observed extended sources in the sky, while the estimation of the PE emission direction is fundamental to determine the polarization of the incoming radiation. The reconstruction of IXPE events can be reduced to the estimation of these two main parameters: (1) the impact point, and (2) the polarization angle ϕ . Currently, an analytic approach is used to infer both the impact point and the polarization angle from the charge-weighted pixel content exploiting a geometrical moments analysis technique. This approach shows its weaknesses by well reconstructing (on average) only $\sim 20\%$ of the events, losing mostly the low-energy ones, which are generally less featured (less elongated tracks, more spot-like). The weakness of the analytical approach brings up the necessity of an alternative reconstruction method and, since the IXPE track reconstruction is based on images, it is very appealing from the deep learning point of view.

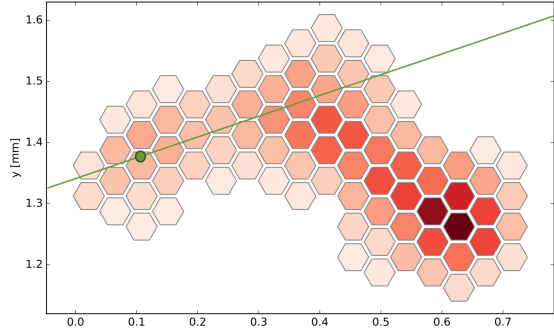


Figure 1: Example of a PE track: The darker the color, the higher the charge value recorded.

Deep learning has successfully been applied in various domains such as medical image analysis, remote sensing, or astronomy (LeCun, Bengio, and Hinton, 2015). In this work, we report results of two first attempts to address the estimation tasks sketched above, i.e., we propose deep neural networks for (1) the impact point estimation and for (2) the estimation of the emission direction. We also outline strategies for further improvements of deep learning based models for both tasks.

2 Data and Reconstruction efficiency

For this study, we simulated IXPE observations of an unpolarized source emitting X-rays of energies uniformly distributed in the range of the IXPE sensitivity. In particular, Monte Carlo simulations were used to generate 500,000 PE track images. Each track image was labelled with the following set of parameters: (1) the energy of the incoming X-ray (E_X), (2) the coordinates (j, i) of the pixel containing the impact point, and (3) the polarization angle ϕ . The generated images were subsequently normalized (i.e., pixel values in $[0,1]$) and upsampled to a cartesian grid (upsampling factor ≈ 2 , equally-shaped square images). In Figure 2, some examples of such generated images are shown. A separate additional test set of 35,838 observations for a $\pi/4$ polarized source emitting X-rays at 4 kilo electronvolts was processed in the same way.

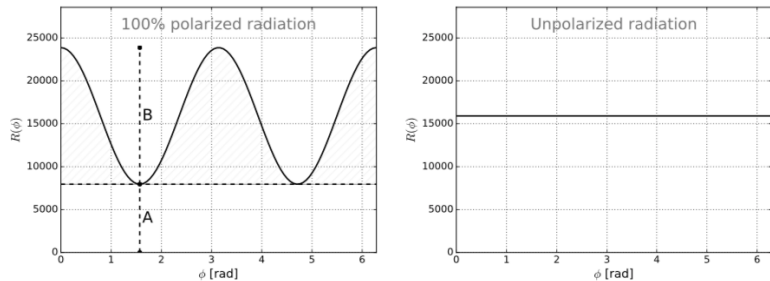


Figure 3: Left: Illustration of a 100% polarized radiation as seen by IXPE. Right: Same as left image but for an unpolarized radiation.

A relevant characteristic is that the distribution of ϕ of the events collected observing an X-ray source in the sky would show a \cos^2 modulation in the case that the target is linearly polarized, while it would be uniform in case of unpolarized source, as illustrated in Figure 3. The capability of an algorithm of reproducing this modulation in the final distribution of ϕ can be translated in an efficiency

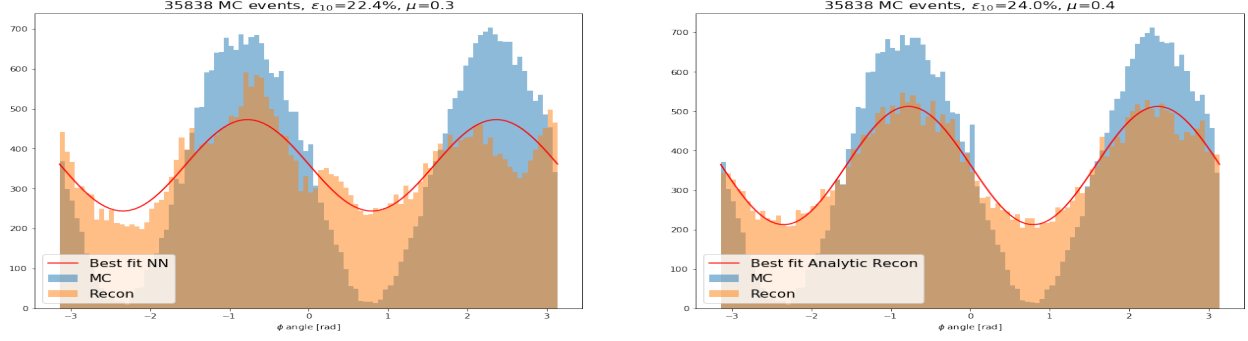


Figure 4: Left: neural network prediction efficiency. Right: state of the art analytical method. The efficiency ϵ_{10} and the modulation factor μ are reported on top of the plots.

evaluation useful to compare reconstruction algorithms. We can define the modulation factor μ as the response to a fully polarized sample: the closer to 1 the modulation factor, the more efficient the algorithm. In addition to the modulation factor, we define the *efficiency*, ϵ_{10} , to compare the performance of different algorithms in predicting ϕ . It is given by the number of events whose predicted polarization angle lies within 10 degrees (arbitrary but reasonable number) of the true value. Given the periodicity of the polarization angle distribution a shifting phase of $\pm\pi$ and $\pm2\pi$ of the reconstructed angle is still good, since the overall distribution would not be altered (as long as the number of positive-shifted events is balanced by the number of negative shifted events).

3 Angle and Impact Estimation

We propose two different neural network architectures to estimate (a) the emission direction (angle) and (b) the impact point of a given track, respectively.

3.1 Polarization Angle Reconstruction

For this subtask, we resort to a M -head ensemble of VGG-16 networks with $M = 8$ heads in the ensemble, where all but the last block of CNN filters are shared (Lee et al., 2015; Simonyan and Zisserman, 2014). The network produces a normalized direction vector and we consider the cosine similarity loss between the network predictions and the ground truth directions as loss function. Following (Lee et al., 2015), we assign a higher weight factor to the loss for the ensemble head, which gives most accurate prediction, and lower weights for the other heads in order to prevent network heads from becoming too similar. At inference stage, the average over ensemble heads is returned as the final prediction.

For typical low energy events accurate direction regression can be impossible, therefore it is important to quantify predictive uncertainty of the model, which we accomplish by using ensembling. It is known that ensembles of neural networks typically yield the best estimate of predictive uncertainty (Ovadia et al., 2019), compared to methods such as dropout (Gal and Ghahramani, 2015) and SVI (Blundell et al., 2015), in addition to improvements in accuracy over single models. In Figure 4, histograms of the reconstructions of the $\pi/4$ -polarized test data together with 10-degree efficiency estimates ϵ_{10} and the modulation factors μ for both the neural network and the classical reconstructions are provided. It can be seen that the baseline model gives nearly the same efficiency as the state-of-the-art analytical method. Ideally, the goal is to outperform the analytical method, and we will discuss potential strategies for that in the conclusion.

3.2 Impact Point Reconstruction

For the impact point estimation task, we resorted to the ResNet-34 model (He et al., 2016) with pre-trained weights (based on ImageNet). That is, we follow a transfer learning approach (Pratt, 1993) and only fine-tune the last layer according to the new task. The image sample are labeled based on the true (simulated) impact point coordinates. For training the last layer, we used 60,000

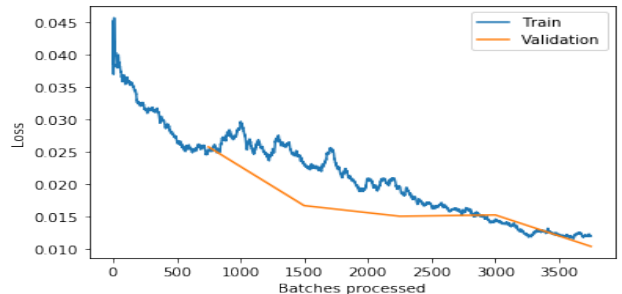


Figure 5: Training and validation loss

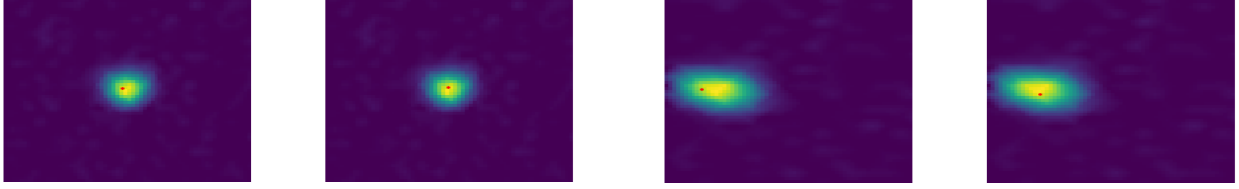


Figure 6: Subfigure 1 and 2 - Left: Ground truth, Right: Regression prediction.

events from the available track samples, 20% samples were used for validation. We obtained 15,000 events separately for the purpose of testing the model.

For training the model, we considered the Mean Square Error (MSE) as the loss function, an initial learning rate of $3e - 2$ with weight decay of $1e - 3$, a batch size of 64, and five epochs. The image size of the samples is 64×64 . The training loss starts with a value of 0.0372 (Figure 5) and later follows a downward path with the increase in the number of batches processed.

The validation loss starts with a similar value of 0.0257 and later decreases steadily. Near the end of the batch processing, the training and the validation loss reach a value of 0.011 and 0.010 respectively. We use Root Mean Square Error (RMSE) as the performance measure and the model showed RMSE in x to be 7.807 whereas RMSE in y as 7.368 for evaluation on test data.

4 Conclusions and Future Work

We have introduced the track reconstruction challenge for the IXPE mission and have shown that existing neural network architectures can achieve results close to the state-of-the-art reconstruction algorithms. In addition to comparable efficiency of the reconstruction, the machine learning techniques provide means of estimating the uncertainties associated to the predicted values, which is an important advantage over the analytic approach, and allows us to set quality cuts on the final reconstructed data, enhancing the accuracy of the IXPE scientific observations. Furthermore, there are multiple directions for further research:

- Firstly, it is worth stressing that the current image pre-processing is not optimal: Since the original images are cropped around the cluster of pixels above the trigger threshold, they exhibit different sizes, meaning that our attempt to produce equally-sized images alters the aspect ratio of the actual tracks.
- Secondly, since the sensor has hexagonal pixels, conventional ‘cartesian’ convolutional filters in fact *do not* yield equivariant feature maps when applied to the raw image data coming from the sensor and can, therefore, lead to a suboptimal performance. For the baseline experiments we used $2 \times$ upsampling to a cartesian grid from the original hexagonal grid, but a better approach would be to use *hexagonal* convolutions instead, which work with raw data and take the actual sensor grid shape into account. Hexagonal convolutions have been implemented, e.g., in the HexagDLy library (Steppa and Holch, 2019) for PyTorch. A further step in this direction would be to investigate hexagonal group convolutions (Cohen and Welling, 2016; Hooigeboom et al., 2018), which capture rotational feature symmetries and result in higher parameter efficiency.
- Thirdly, model calibration should be improved as well. We see in Figure 4 that, compared to the neural network, the analytical method results in a very clear sinusoidal shape of the histogram. Increasing the ensemble size and using alternative methods for sampling from the posterior distribution of directions could potentially reduce the irregularities for the neural network reconstructions. A possible improvement could be achieved by adding the information about the location of the impact point as input parameters in addition to the images.
- Finally, the basic direction regression and hit point detection tasks can be combined in a single model for simultaneous prediction on both tasks, as is typically done for *multi-task learning* (Ruder, 2017) tasks. Multi-task learning, intuitively, adds additional supervision signals to the network, and such additional signals could lead to an overall model outperforming the individual models trained exclusively for single tasks.

We plan to investigate the aforementioned extensions and research directions in the near future.

5 Acknowledgements

We want to thank the DarkMachines collaboration for bringing us together and for fruitful discussions. Michela Negro wants to acknowledge the IXPE team and in particular Niccoló Di Lalla and Alberto Manfreda for providing the simulated data samples.

References

- [1] R. Bellazzini et al. “Gas pixel detectors for X-ray polarimetry applications”. In: *Nuclear Instruments and Methods in Physics Research A* 560.2 (May 2006), pp. 425–434. DOI: 10.1016/j.nima.2006.01.046. arXiv: astro-ph/0512242 [astro-ph].
- [2] Charles Blundell et al. “Weight Uncertainty in Neural Networks”. In: *arXiv e-prints*, arXiv:1505.05424 (May 2015), arXiv:1505.05424. arXiv: 1505.05424 [stat.ML].
- [3] Taco S. Cohen and Max Welling. “Group Equivariant Convolutional Networks”. In: *CoRR abs/1602.07576* (2016). arXiv: 1602.07576. URL: <http://arxiv.org/abs/1602.07576>.
- [4] Enrico Costa et al. “An efficient photoelectric X-ray Polarimeter for the study of Black Holes and Neutron Stars”. In: *Nature* 411 (July 2001), pp. 662–5. DOI: 10.1038/35079508.
- [5] Yarin Gal and Zoubin Ghahramani. “Dropout as a Bayesian Approximation: Representing Model Uncertainty in Deep Learning”. In: *arXiv e-prints*, arXiv:1506.02142 (June 2015), arXiv:1506.02142. arXiv: 1506.02142 [stat.ML].
- [6] Kaiming He et al. “Deep residual learning for image recognition”. In: *Proceedings of the IEEE conference on computer vision and pattern recognition*. 2016, pp. 770–778.
- [7] Emiel Hoogeboom et al. “HexaConv”. In: *CoRR abs/1803.02108* (2018). arXiv: 1803.02108. URL: <http://arxiv.org/abs/1803.02108>.
- [8] Yann LeCun, Yoshua Bengio, and Geoffrey Hinton. “Deep Learning”. In: *Nature* 521 (7553 2015), pp. 436–444.
- [9] Stefan Lee et al. “Why M Heads are Better than One: Training a Diverse Ensemble of Deep Networks”. In: *CoRR abs/1511.06314* (2015). arXiv: 1511.06314. URL: <http://arxiv.org/abs/1511.06314>.
- [10] Yaniv Ovadia et al. “Can You Trust Your Model’s Uncertainty? Evaluating Predictive Uncertainty Under Dataset Shift”. In: *arXiv e-prints*, arXiv:1906.02530 (June 2019), arXiv:1906.02530. arXiv: 1906.02530 [stat.ML].
- [11] Lorian Y Pratt. “Discriminability-based transfer between neural networks”. In: *Advances in neural information processing systems*. 1993, pp. 204–211.
- [12] Sebastian Ruder. “An Overview of Multi-Task Learning in Deep Neural Networks”. In: *CoRR abs/1706.05098* (2017). arXiv: 1706.05098. URL: <http://arxiv.org/abs/1706.05098>.
- [13] Karen Simonyan and Andrew Zisserman. “Very Deep Convolutional Networks for Large-Scale Image Recognition”. In: *arXiv e-prints*, arXiv:1409.1556 (Sept. 2014), arXiv:1409.1556. arXiv: 1409.1556 [cs.CV].
- [14] Constantin Steppa and Tim L. Holch. “HexagDLy—Processing hexagonally sampled data with CNNs in PyTorch”. In: *SoftwareX* 9 (2019), pp. 193–198. ISSN: 2352-7110. DOI: <https://doi.org/10.1016/j.softx.2019.02.010>. URL: <https://www.sciencedirect.com/science/article/pii/S2352711018302723>.
- [15] Martin C. Weisskopf. “An Overview of X-Ray Polarimetry of Astronomical Sources”. In: *Galaxies* 6.1 (2018). ISSN: 2075-4434. DOI: 10.3390/galaxies6010033. URL: <https://www.mdpi.com/2075-4434/6/1/33>.